Journal of the Egyptian Mathematical Society (2016) 24, 92–99

Egyptian Mathematical Society

Journal of the Egyptian Mathematical Society

www.etms-eg.org
www.elsevier.com/locate/joems

ORIGINAL ARTICLE

Wave propagation in a transversely isotropic magneto-electro-elastic solid bar immersed in an inviscid fluid

R. Selvamani [a,*], P. Ponnusamy [b]

[a] Department of Mathematics, Karunya University, Coimbatore, Tamil Nadu, India
[b] Departments of Mathematics, Govt Arts College, Coimbatore, Tamil Nadu, India

Received 5 November 2013; revised 11 March 2014; accepted 18 June 2014
Available online 19 July 2014

KEYWORDS

Electro-magnetic waves;
Solid–fluid interface;
Electro-magneto-elastic bar/plate;
Transducers;
Sensors/actuators;
MEMS/NEMS

Abstract Wave propagation in a transversely isotropic magneto-electro-elastic solid bar immersed in an inviscid fluid is discussed within the frame work of linearized three dimensional theory of elasticity. Three displacement potential functions are introduced to uncouple the equations of motion, electric and magnetic induction. The frequency equations that include the interaction between the solid bar and fluid are obtained by the perfect slip boundary conditions using the Bessel functions. The numerical calculations are carried out for the non-dimensional frequency, phase velocity and attenuation coefficient by fixing wave number and are plotted as the dispersion curves. The results reveal that the proposed method is very effective and simple and can be applied to other bar of different cross section by using proper geometric relation.

2010 MATHEMATICS SUBJECT CLASSIFICATION: 73B; 73C; 73D; 76W; 49M

1. Introduction

The smart composite material such as a magneto-electro-elastic material exhibits the desirable coupling effect between electric and magnetic fields and has gained considerable importance since last decade. These materials have the capacity to convert one form of energy namely, magnetic, electric and mechanical energy to another form of energy. The composite consisting of piezoelectric and piezomagnetic components has found increasing application in engineering structures, particularly in smart/intelligent structure system. In addition, magnetoelectroelastic materials have been used extensively in the design of light weighted and high performance sensors and transducers due to direct and converse piezoelectricity effects. The direct piezoelectric effect is used in sensing applications, such as in force or displacement sensors. The converse piezoelectric effects are used in transduction applications, such as in motors and device that precisely control positioning, and in generating sonic and ultrasonic signals. This study may be used in applications involving nondestructive testing (NDT), qualitative

* Corresponding author. Tel.: +91 9842647487.
E-mail address: selvam1729@gmail.com (R. Selvamani).

Peer review under responsibility of Egyptian Mathematical Society.

Production and hosting by Elsevier

http://dx.doi.org/10.1016/j.joems.2014.06.016
1110-256X © 2014 Production and hosting by Elsevier B.V. on behalf of Egyptian Mathematical Society.

nondestructive evaluation (QNDE) of large diameter pipes and health monitoring of other ailing infrastructures in addition to check and verify the validity of FEM and BEM for such problems.

Pan [1] and Pan and Heyliger [2] have discussed the three-dimensional behavior of magnetoelectroelastic laminates under simple support. An exact solution for magnetoelectroelastic laminates in cylindrical bending has also been obtained by Pan and Heyliger [3]. Pan and Han [4] derived the exact solution for functionally graded and layered magneto-electro-elastic plates. Feng and Pan [5] discussed the dynamic fracture behavior of an internal interfacial crack between two dissimilar magneto-electro-elastic plates. Buchanan [6] developed the free vibration of an infinite magneto-electro-elastic cylinder. Dai and Wang [7,8] have studied thermo-electro-elastic transient responses in piezoelectric hollow structures and hollow cylinder subjected to complex loadings.

Later Wang with Kong et al. [9] presented the thermo-magneto-dynamic stresses and perturbation of magnetic field vector in a non-homogeneous hollow cylinder. Annigeri et al. [10–12] studied respectively, the free vibration of clamped-clamped magneto-electro-elastic cylindrical shells, free vibration behavior of multiphase and layered magneto-electro-elastic beam, free vibrations of simply supported layered and multiphase magneto-electro-elastic cylindrical shells. Hon et al. [13] analyzed a point heat source on the surface of semi-infinite transversely isotropic electro-magneto-thermo-elastic materials. Sharma and Mohinder Pal [14] developed the Rayleigh-Lamb waves in magneto-thermo-elastic homogeneous isotropic plate. Later Sharma and Thakur [15] studied the effect of rotation on Rayleigh-Lamb waves in magneto-thermo-elastic media. Gao and Noda [16] presented the thermal-induced interfacial cracking of magnetoelectroelastic materials. Bin et al. [17] studied the wave propagation in non-homogeneous magneto-electo-elastic plates.

Sinha et al. [18] made an investigation about the axisymmetric wave propagation in circular cylindrical shell immersed in a fluid, in two parts. In Part I, the theoretical analysis of the propagation modes is discussed and in Part II, the axisymmetric modes excluding tensional modes are obtained both theoretically and experimentally and are compared. Berliner and Solecki [19] investigated wave propagation in a fluid loaded transversely isotropic cylinder. In that paper, Part I consists of the analytical formulation of the frequency equation of the coupled system consisting of the cylinder with inner and outer fluid and Part II gives the numerical results.

Ponnusamy [20] has studied the wave propagation in a generalized thermoelastic cylinder of arbitrary cross-section immersed in a fluid using the Fourier expansion collocation method. Recently, Ponnusamy and Selvamani [21,22] have studied respectively, the three dimensional wave propagation of transversely isotropic magneto thermo elastic and generalized thermo elastic cylindrical panel in the context of the linear theory of thermo elasticity.

In this problem, the wave propagation in a transversely isotropic magneto-electro-elastic solid bar immersed in an inviscid fluid is studied using Bessel function. Three displacement potential functions, electric field vector and magnetic fields are used to uncouple the equations of motion. The frequency equations are obtained from the perfect slip boundary conditions. The computed non-dimensional frequencies, phase velocity and attenuation coefficient are plotted in the form of dispersion curves and their characteristics are discussed.

2. Formulation of the problem

The constitutive equations of a transversely isotropic linear magneto-electro-elastic material, involving stresses σ_j, strain S_{ij}, electric displacements D_{ij}, electric field E_k, magnetic induction B_j and magnetic field H_k are considered in the lines of Buchannan [6],

$$\sigma_j = C_{jk}S_k - e_{jk}E_k - q_{kj}H_k \tag{1}$$

$$D_j = e_{jk}S_k + \varepsilon_{jk}E_k + m_{jk}H_k \tag{2}$$

$$B_j = q_{jk}S_k + m_{jk}E_k + \mu_{jk}H_k \tag{3}$$

where C_{jk},ε_{jk} and μ_{jk} are the elastic, dielectric and magnetic permeability coefficients respectively; e_{kj}, q_{kj} and m_{jk} are the piezoelectric, piezomagnetic and magnetoelectric material coefficients.

The strain S_{ij} is related to the displacements corresponding to the cylindrical coordinates (r, θ, z) which are given by

$$S_{rr} = \frac{\partial u_r}{\partial r}, \quad S_{\theta\theta} = \frac{1}{r}\left(u_r + \frac{\partial u_\theta}{\partial \theta}\right), \quad S_{zz} = \frac{\partial u_z}{\partial z}$$
$$S_{r\theta} = \left(\frac{1}{r}\frac{\partial u_r}{\partial \theta} + \frac{\partial u_\theta}{\partial r} - \frac{u_\theta}{r}\right), S_{rz} = \left(\frac{\partial u_z}{\partial r} + \frac{\partial u_r}{\partial z}\right),$$
$$S_{\theta z} = \left(\frac{1}{r}\frac{\partial u_z}{\partial \theta} + \frac{\partial u_\theta}{\partial z}\right) \tag{4}$$

where u_r,u_θ and u_z are the mechanical displacements corresponding to the cylindrical coordinate directions r, θ and z. The relation between the electric field vector E_i and the electric potential ϕ is given by

$$E_r = -\frac{\partial \phi}{\partial r}, \quad E_\theta = -\frac{1}{r}\frac{\partial \phi}{\partial \theta} \text{ and } E_z = -\frac{\partial \phi}{\partial z} \tag{5}$$

Similarly, the magnetic field H_i is related to the magnetic potential ψ as

$$H_r = -\frac{\partial \psi}{\partial r}, \quad H_\theta = -\frac{1}{r}\frac{\partial \psi}{\partial \theta} \text{ and } H_z = -\frac{\partial \psi}{\partial z} \tag{6}$$

The basic governing equations of motion, electrostatic displacement D_j and magnetic induction B_j in cylindrical co-ordinates (r, θ, z) system, in the absence of volume force are

$$\frac{\partial \sigma_{rr}}{\partial r} + \frac{1}{r}\frac{\partial \sigma_{r\theta}}{\partial \theta} + \frac{\partial \sigma_{rz}}{\partial z} + \frac{1}{r}(\sigma_{rr} - \sigma_{\theta\theta}) = \rho\frac{\partial^2 u_r}{\partial t^2} \tag{7a}$$

$$\frac{\partial \sigma_{\theta r}}{\partial r} + \frac{1}{r}\frac{\partial \sigma_{\theta\theta}}{\partial \theta} + \frac{\partial \sigma_{\theta z}}{\partial z} + \frac{2\sigma_{\theta r}}{r} = \rho\frac{\partial^2 u_\theta}{\partial t^2} \tag{7b}$$

$$\frac{\partial \sigma_{zr}}{\partial r} + \frac{1}{r}\frac{\partial \sigma_{z\theta}}{\partial \theta} + \frac{\partial \sigma_{zz}}{\partial z} + \frac{\sigma_{rz}}{r} = \rho\frac{\partial^2 u_z}{\partial t^2} \tag{7c}$$

$$\frac{\partial D_r}{\partial r} + \frac{D_r}{r} + \frac{\partial D_\theta}{\partial \theta} + \frac{\partial D_z}{\partial z} = 0 \tag{7d}$$

$$\frac{\partial B_r}{\partial r} + \frac{B_r}{r} + \frac{\partial B_\theta}{\partial \theta} + \frac{\partial B_z}{\partial z} = 0 \tag{7e}$$

where the stress strain relation for the transversely isotropic medium is given by

$$\sigma_{rr} = c_{11}S_{rr} + c_{12}S_{\theta\theta} + c_{13}S_{zz} - e_{31}E_z - q_{31}H_z \tag{8a}$$
$$\sigma_{\theta\theta} = c_{12}S_{rr} + c_{11}S_{\theta\theta} + c_{13}S_{zz} - e_{31}E_z - q_{31}H_z \tag{8b}$$
$$\sigma_{zz} = c_{13}S_{rr} + c_{13}S_{\theta\theta} + c_{33}S_{zz} - e_{33}E_z - q_{33}H_z \tag{8c}$$
$$\sigma_{r\theta} = c_{66}S_{r\theta} \tag{8d}$$
$$\sigma_{\theta z} = c_{44}S_{\theta z} - e_{15}E_\theta - q_{15}H_\theta \tag{8e}$$
$$\sigma_{rz} = c_{44}S_{rz} - e_{15}E_r - q_{15}H_r \tag{8f}$$

The electric displacement and magnetic induction are related in terms of strain, electric field and magnetic field in the following form.

$$D_r = e_{15}S_{rz} + \varepsilon_{11}E_r + m_{11}H_r \tag{9a}$$
$$D_\theta = e_{15}S_{\theta z} + \varepsilon_{11}E_\theta + m_{11}H_\theta \tag{9b}$$
$$D_z = e_{31}(S_{rr} + S_{\theta\theta}) + e_{33}S_{zz} + \varepsilon_{33}E_z + m_{33}H_z \tag{9c}$$

$$B_r = q_{15}S_{rz} + m_{11}E_r + \mu_{11}H_r \tag{10a}$$
$$B_\theta = q_{15}S_{\theta z} + m_{11}E_\theta + \mu_{11}H_\theta \tag{10b}$$
$$B_z = q_{31}(S_{rr} + S_{\theta\theta}) + q_{33}S_{zz} + m_{33}E_z + \mu_{33}H_z \tag{10c}$$

Substitution of Eqs. (4)–(6) along with Eqs. (8)–(10) into Eqs. (7) we obtain the following set of governing equations in terms of displacements, electric potential and magnetic potential as

$$\begin{aligned} &c_{11}\left(u_{r,rr} + r^{-1}u_{r,r} - r^{-2}u_r\right) + c_{66}r^{-2}u_{r,\theta\theta} + c_{44}u_{r,zz} \\ &\quad + (c_{66} + c_{12})r^{-1}u_{\theta,r\theta} - (c_{11} + c_{66})r^{-2}u_{\theta,\theta} + (c_{44} + c_{13})u_{z,rz} \\ &\quad + (e_{31} + e_{15})\phi_{,rz} + (q_{31} + q_{15})\phi_{,rz} = \rho u_{r,tt} \end{aligned} \tag{11a}$$

$$\begin{aligned} &(c_{66}+c_{12})r^{-1}u_{r,r\theta} + (c_{11}+c_{66})r^{-2}u_{r,\theta} + c_{66}\left(u_{\theta,rr} + r^{-1}u_{\theta,r} - r^{-2}u_\theta\right) \\ &\quad + c_{44}u_{\theta,zz} + c_{11}r^{-2}u_{\theta,\theta\theta} + (c_{44}+c_{13})r^{-1}u_{z,\theta z} \\ &\quad + (e_{31}+e_{15})r^{-1}\phi_{,\theta z} + (q_{31}+q_{15})\psi_{,\theta z} = \rho u_{\theta,tt} \end{aligned} \tag{11b}$$

$$\begin{aligned} &(c_{44} + c_{13})\left(u_{r,rz} + r^{-1}u_{r,z} + r^{-1}u_{\theta,\theta z}\right) + c_{44}\left(u_{z,rr} + r^{-1}u_{z,r} + u_{z,\theta\theta}\right) \\ &\quad + c_{33}u_{z,zz} + e_{33}\phi_{,zz} + q_{33}\psi_{,zz} + e_{15}\left(\phi_{,rr} + r^{-1}\phi_{,r} + \phi_{,\theta\theta}\right) \\ &\quad + q_{15}\left(\psi_{,rr} + r^{-1}\psi_{,r} + \psi_{,\theta\theta}\right) = \rho u_{z,tt} \end{aligned} \tag{11c}$$

$$\begin{aligned} &e_{15}\left(u_{z,rr} + r^{-1}u_{z,r} + r^{-2}u_{z,\theta\theta}\right) + (e_{31} + e_{15})\left(u_{r,rz} + r^{-1}u_{r,z} + r^{-1}u_{\theta,\theta z}\right) \\ &\quad + e_{33}u_{z,zz} - \varepsilon_{33}\phi_{,zz} - m_{33}\psi_{,zz} - \varepsilon_{11}\left(\phi_{,rr} + r^{-1}\phi_{,r} + \phi_{,\theta\theta}\right) \\ &\quad - m_{11}\left(\psi_{,rr} + r^{-1}\psi_{,r} + \psi_{,\theta\theta}\right) = 0 \end{aligned} \tag{11d}$$

$$\begin{aligned} &q_{15}\left(u_{z,rr} + r^{-1}u_{z,r} + u_{z,\theta\theta}\right) + (q_{31} + q_{15})\left(u_{r,rz} + r^{-1}u_{r,z} + r^{-1}u_{\theta,\theta z}\right) \\ &\quad + q_{33}u_{z,zz} - \mu_{33}\psi_{,zz} - m_{33}\phi_{,zz} - \mu_{11}\left(\psi_{,rr} + r^{-1}\psi_{,r} + \psi_{,\theta\theta}\right) \\ &\quad - m_{11}\left(\phi_{,rr} + r^{-1}\phi_{,r} + \phi_{,\theta\theta}\right) = 0 \end{aligned} \tag{11e}$$

3. Method of solution of the solid medium

Eqs. (11a)–(11e) are coupled with both odd ordered and even ordered derivatives of three displacements, electric potential and magnetic potential components with respect to one specific coordinate variable. To uncouple Eq. (11) we seek the solution in the following form:

$$\begin{aligned} u_r(r,\theta,z,t) &= \left[\left(\phi_{,r} + r^{-1}\psi_{,\theta}\right) + \left(\bar{\phi}_{,r} + r^{-1}\bar{\psi}_{,\theta}\right)\right]e^{i(kz+\omega t)} \\ u_\theta(r,\theta,z,t) &= \left[\left(r^{-1}\phi_{,\theta} - \psi_{,r}\right) + \left(r^{-1}\bar{\phi}_{,\theta} - \bar{\psi}_{,r}\right)\right]e^{i(kz+\omega t)} \\ u_z(r,\theta,z,t) &= \frac{i}{a}(W + \overline{W})e^{i(kz+\omega t)} \\ \Phi(r,\theta,z,t) &= \frac{i}{a}\left(\frac{c_{44}}{e_{33}}\right)(\Phi + \overline{\Phi})e^{i(kz+\omega t)} \\ \Psi(r,\theta,z,t) &= \frac{i}{a}\left(\frac{c_{44}}{e_{33}}\right)(\Psi + \overline{\Psi})e^{i(kz+\omega t)} \end{aligned} \tag{12}$$

where $i = \sqrt{-1}$, k is the wave number, ω is the angular frequency, $\phi(r,\theta)$, $\psi(r,\theta)$, $W(r,\theta)$, $\Phi(r,\theta)$ and $\Psi(r,\theta)$ are the displacement potentials for symmetric modes of vibrations and the bared quantities $\bar{\phi}(r,\theta), \bar{\psi}(r,\theta), \overline{W}(r,\theta), \overline{\Phi}(r,\theta)$ and $\overline{\Psi}(r,\theta)$ represents the displacement potentials for anti symmetric modes of vibration, a is the geometrical parameter of the cylindrical bar.

Introducing the dimensionless quantities such as

$$\begin{aligned} &\varsigma = ka, \quad x = \frac{r}{a}, \quad \Omega = \omega a/c_1^2, \quad \bar{c}_{ij} = \frac{c_{ij}}{c_{44}}, \\ &\bar{e}_{ij} = \frac{e_{ij}}{e_{33}}, \quad \bar{q}_{ij} = \frac{q_{ij}}{q_{33}}, \quad \bar{m}_{ij} = \frac{m_{ij}c_{44}}{e_{33}q_{33}} \quad \bar{\varepsilon}_{ij} = \frac{\varepsilon_{ij}c_{44}}{e_{33}^2}, \\ &\bar{\mu}_{ij} = \frac{\mu_{ij}c_{44}}{q_{33}^2}, \quad c_1^2 = \frac{c_{44}}{\rho}, \quad T_a = \sqrt{c_{11}/\rho}/a, \quad \bar{z} = z/a \end{aligned} \tag{13}$$

and substituting Eqs. (12) and (13) into Eqs. (11a)–(11e), we obtain

$$\begin{aligned} &[\bar{c}_{11}\nabla^2 + (\Omega^2 - \varsigma^2)]\phi - \varsigma(1 + \bar{c}_{13})W - \varsigma(\bar{e}_{13} + \bar{e}_{15})\Phi \\ &\quad - \varsigma(\bar{q}_{31} + \bar{q}_{15})\Psi = 0 \end{aligned} \tag{14a}$$
$$\begin{aligned} &\varsigma(1 + \overline{c_{13}})\nabla^2\phi + \left[\nabla^2 + \Omega^2 - \varsigma^2\overline{c_{33}}\right]W + \left(\overline{e_{15}}\nabla^2 - \varsigma^2\right)\Phi \\ &\quad + \left(\overline{q_{15}}\nabla^2 - \varsigma^2\right)\Psi = 0 \end{aligned} \tag{14b}$$
$$\begin{aligned} &\varsigma(\overline{e_{31}} + \overline{e_{15}})\nabla^2\phi + \left(\overline{e_{15}}\nabla^2 - \varsigma^2\right)W - \left(\overline{\varepsilon_{11}}\nabla^2 - \varsigma^2\overline{\varepsilon_{33}}\right)\Phi \\ &\quad - \left(\overline{m_{11}}\nabla^2 - \varsigma^2\overline{m_{33}}\right)\Psi = 0 \end{aligned} \tag{14c}$$
$$\begin{aligned} &\varsigma(\overline{q_{31}} + \overline{q_{15}})\nabla^2\phi + \left(\overline{q_{15}}\nabla^2 - \varsigma^2\right)W - \left(\overline{m_{11}}\nabla^2 - \varsigma^2\overline{m_{33}}\right)\Phi \\ &\quad - \left(\overline{\mu_{11}}\nabla^2 - \varsigma^2\overline{\mu_{33}}\right)\Psi = 0 \end{aligned} \tag{14d}$$

and

$$\left(\nabla^2 + \frac{(\Omega^2 - \varsigma^2)}{\overline{c_{66}}}\right)\Psi = 0 \tag{15}$$

where $\nabla^2 = \frac{\partial^2}{\partial x^2} + \frac{1}{x}\frac{\partial}{\partial x} + \frac{1}{x^2}\frac{\partial^2}{\partial \theta^2}$

For the existence of non-trivial solution of Eqs. (14a)– (14d), the determinant of the coefficient of the system is set to zero

$$\begin{vmatrix} \bar{c}_{11}\nabla^2 + \Omega^2 - \varsigma^2 & -\varsigma(1 + \bar{c}_{13}) & -\varsigma(\bar{e}_{31} + \bar{e}_{15}) & -\varsigma(\bar{q}_{31} + \bar{q}_{15}) \\ \varsigma(1 + \bar{c}_{13})\nabla^2 & (\nabla^2 + \Omega^2 - \varsigma^2\bar{c}_{33}) & (\bar{e}_{15}\nabla^2 - \varsigma^2) & (\bar{q}_{15}\nabla^2 - \varsigma^2) \\ \varsigma(\bar{e}_{31} + \bar{e}_{15})\nabla^2 & (\bar{e}_{15}\nabla^2 - \varsigma^2) & (\varsigma^2\bar{\varepsilon}_{33} - \bar{\varepsilon}_{11}\nabla^2) & (\bar{m}_{33}\varsigma^2 - \bar{m}_{11}\nabla^2) \\ \varsigma(\bar{q}_{31} + \bar{q}_{15})\nabla^2 & (\bar{q}_{15}\nabla^2 - \varsigma^2) & (\bar{m}_{33}\varsigma^2 - \bar{m}_{11}\nabla^2) & (\bar{\mu}_{33}\varsigma^2 - \bar{\mu}_{11}\nabla^2) \end{vmatrix}(\phi, W, \Phi, \Psi) = 0 \tag{16}$$

The above determinant Eq. (16) results in an ordinary differential equation as follows

$$(A\nabla^8 + B\nabla^6 + C\nabla^4 + D\nabla^2 + E)(\phi, W, \Phi, \Psi) = 0 \quad (17)$$

where the coefficients occurring in Eq. (17) are

$$A = \bar{c}_{11} g_1$$

$$\begin{aligned} B = {} & \bar{c}_{11}\left[g_2 + g_3 g_4 - g_5 - 2\bar{e}_{15} g_6 + 2\bar{q}_{15} g_7 + 2\varsigma^2 \bar{e}_{15}\bar{q}_{15}\bar{m}_{33}\right] \\ & + g_8 g_2 + g_9^2 g_4 + 2\varsigma g_9 g_{10} g_{11} + 2\varsigma g_9 g_{12} g_{13} + \varsigma^2 g_{10}^2 g_{14} \\ & + 2\varsigma^2 g_{10} g_{12} g_{15} - \varsigma^2 g_{12}^2 g_{16} \end{aligned}$$

$$\begin{aligned} C = {} & \bar{c}_{11}\left[\varsigma^2 g_{17} + g_3 g_2 - 2\bar{e}_{15}\varsigma^2 g_{18} + \varsigma^2 (g_6 - g_7) - 2\varsigma^2 \bar{q}_{15} g_{19}\right] \\ & + g_8\left[g_2 + g_3 g_4 - g_5 - 2\overline{e_{15}} g_6 + 2\bar{q}_{15} g_7 + 2\varsigma^2 \bar{e}_{15}\bar{q}_{15}\bar{m}_{33}\right] \\ & + g_9^2 g_2 + 2\varsigma g_9 g_{10}(g_6 - g_{20}) + 2\varsigma g_9 g_{12}(g_7 + g_{21}) + \varsigma^4 g_{10}^2 g_{22} \\ & - 2\varsigma^4 g_{10} g_{12} g_{23} - \varsigma^2 \bar{e}_{15} g_{10}^2 g_3 + 2\varsigma^2 \bar{m}_{11} g_{10} g_{12} g_3 + \varsigma^4 g_{12}^2 g_{25} \\ & - \varsigma^2 \bar{\varepsilon}_{11} g_{12}^2 g_3 \end{aligned}$$

$$\begin{aligned} D = {} & \bar{c}_{11}\left[\varsigma^2 g_{17} g_3 + \varsigma^4 (g_{18} - g_{19})\right] \\ & + g_8\left[\varsigma^2 g_{17} + g_2 g_3 - 2\bar{e}_{15}\varsigma^2 g_{18} + \varsigma^2 (g_6 - g_7) - 2\varsigma^2 \bar{q}_{15} g_{19}\right] \\ & + \varsigma^4 g_9^2 g_{24} - 2\varsigma^3 g_{10} g_9 g_{18} - 2\varsigma^3 g_9 g_{12} g_{19} + \varsigma^4 \bar{\mu}_{33} g_{10}^2 g_3 \\ & - 2\varsigma^4 \bar{m}_{33} g_{10} g_{12} g_3 - \varsigma^6 g_{10}^2 + 2\varsigma^6 g_{10} g_{12} + \varsigma^4 \bar{\varepsilon}_{33} g_{12}^2 g_3 - \varsigma^6 g_{12}^2 \end{aligned}$$

$$E = g_8\left[\varsigma^2 g_{17} g_3 + \varsigma^4 (g_{18} - g_{19})\right] \quad (18)$$

where

$$g_1 = \bar{\varepsilon}_{11}\bar{\mu}_{11} - \bar{m}_{11}^2 + \bar{e}_{15}^2 \bar{\mu}_{11}^2 + \bar{q}_{15}^2 \bar{\varepsilon}_{11} - 2\bar{e}_{15}\bar{q}_{15}\bar{m}_{11},$$
$$g_2 = \varsigma^2 (2\bar{m}_{11}\bar{m}_{33} - \bar{\varepsilon}_{33}\bar{\mu}_{11} - \bar{\varepsilon}_{11}\bar{\mu}_{33}), g_3 = \Omega^2 - \varsigma^2 \bar{\varepsilon}_{33},$$
$$g_4 = \bar{\varepsilon}_{11}\bar{\mu}_{11} - \bar{m}_{11}^2, g_5 = \varsigma^2\left(\bar{e}_{15}^2 \bar{\mu}_{33}^2 + \bar{q}_{15}^2 \bar{\varepsilon}_{33}\right), g_6 = \varsigma^2 (\bar{\mu}_{11} - \bar{m}_{11}),$$
$$g_7 = \varsigma^2 (\bar{m}_{11} - \bar{\varepsilon}_{11}), g_8 = \Omega^2 - \varsigma^2, g_9 = \varsigma(1 + \bar{\varepsilon}_{13}),$$
$$g_{10} = \bar{e}_{31} + \bar{e}_{15}, g_{11} = \bar{e}_{15}\bar{\mu}_{11} - \bar{q}_{15}\bar{m}_{11}, g_{12} = \bar{q}_{31} + \bar{q}_{15},$$
$$g_{13} = \bar{q}_{15}\bar{\varepsilon}_{11} - \bar{e}_{15}\bar{m}_{11}, g_{14} = \bar{\mu}_{11} + \bar{q}_{15}^2, g_{15} = \bar{m}_{11} + \bar{e}_{15}\bar{q}_{15},$$
$$g_{16} = \bar{\varepsilon}_{11} + \bar{q}_{15}^2, g_{17} = \varsigma^2\left(\bar{\varepsilon}_{33}\bar{\mu}_{33} - \bar{m}_{33}^2\right), g_{18} = \varsigma^2 (\bar{m}_{33} - \bar{\mu}_{33}),$$
$$g_{19} = \varsigma^2 (\bar{m}_{33} - \bar{\varepsilon}_{33}), g_{20} = \varsigma^2 (\bar{e}_{15}\bar{\mu}_{33} - \bar{m}_{33}\bar{q}_{15}),$$
$$g_{21} = \varsigma^2 (\bar{e}_{15}\bar{m}_{33} - \bar{\varepsilon}_{33}\bar{q}_{15}), g_{22} = \bar{\mu}_{33} + 2\bar{q}_{15},$$
$$g_{23} = \bar{m}_{33} + \bar{q}_{15} + \bar{e}_{15}, g_{23} = \bar{m}_{33} + \bar{q}_{15} + \bar{e}_{15},$$
$$g_{24} = \bar{\varepsilon}_{33}\bar{\mu}_{33} - \bar{m}_{33}^2, g_{25} = \bar{\varepsilon}_{33} + 2\bar{e}_{15}$$

Solving the partial differential equation given in Eq. (17), we obtain the solution as

$$\phi = \sum_{j=1}^{4} A_j J_n(\alpha_j r) \cos n\theta$$

$$W = \sum_{j=1}^{4} a_j A_j J_n(\alpha_j r) \cos n\theta$$

$$\Phi = \sum_{j=1}^{4} b_j A_j J_n(\alpha_j r) \cos n\theta$$

$$\psi = \sum_{j=1}^{4} c_j A_j J_n(\alpha_j r) \cos n\theta \quad (19)$$

Hence, $(\alpha_j r)^2 (j = 1,2,3,4)$ are the non-zero roots of the equation

$$(A\alpha^8 - B\alpha^6 + C\alpha^4 - D\alpha^3 + E) = 0 \quad (20)$$

The solutions corresponding to the root $(\alpha_j a)^2 = 0$ are not considered here, since $J_n(0)$ are zero, except for $n = 0$. The Bessel function J_n is used when the roots $(\alpha_j a)^2 (j = 1, \ldots, 4)$ are real or complex and the modified Bessel function I_n is used when the roots $(\alpha_j\, a)^2 (j = 1,2,3,4)$ are imaginary.

The constants a_j, b_j and c_j defined in Eq. (19) can be calculated from the following equations.

$$\begin{aligned} & \varsigma(1+\bar{c}_{13})a_j + \varsigma(\bar{e}_{31}+\bar{e}_{15})b_j + \varsigma(\bar{q}_{31}+\bar{q}_{15})c_j = \Omega^2 - \varsigma^2 - \bar{c}_{11}(\alpha_j a)^2 \\ & \left((\alpha_j a)^2 + \varsigma^2 \bar{c}_{33} - \Omega^2\right)a_j + \left((\alpha_j a)^2 \bar{e}_{15} + \varsigma^2\right)b_j \\ & \quad + \left((\alpha_j a)^2 \bar{q}_{15} + \varsigma^2\right)c_j = -\varsigma(1+\bar{c}_{13})(\alpha_j a)^2 \\ & \left((\alpha_j a)^2 \bar{e}_{15} + \varsigma^2\right)a_j - \left(\bar{\varepsilon}_{11}(\alpha_j a)^2 + \varsigma^2 \bar{\varepsilon}_{33}\right)b_j \\ & \quad - \left(\bar{m}_{11}(\alpha_j a)^2 + \varsigma^2 \bar{m}_{33}\right)c_j = -\varsigma(\bar{e}_{31}+\bar{e}_{15})(\alpha_j a)^2 \end{aligned} \quad (21)$$

Solving Eq. (15), we obtain

$$\Psi = A_5 J_n(\alpha_5 r) \sin n\theta \quad (22)$$

where $(\alpha_5 a)^2 = \Omega^2 - \zeta^2$. If $(\alpha_5 a)^2 < 0$, the Bessel function J_n is replaced by the modified Bessel function I_n.

4. Equations of motion of the fluid

In cylindrical polar coordinates r,θ and z the acoustic pressure and radial displacement equation of motion for an invicid fluid are of the form Berliner and Solecki [19].

$$p^f = -B^f\left(u^f_{r,r} + r^{-1}\left(u^f_r + u^f_{\theta,\theta}\right) + u^f_{z,z}\right) \quad (23)$$

and

$$\bar{c}_f^2 u^f_{r,tt} = \Delta_{,r} \quad (24)$$

respectively, where B^f is the adiabatic bulk modulus, ρ^f is the density, $c_f = \sqrt{B^f/\rho^f}$ is the acoustic phase velocity in the fluid, and

$$\Delta = \left(u^f_{r,r} + r^{-1}\left(u^f_r + u^f_{\theta,\theta}\right) + u^f_{z,z}\right) \quad (25)$$

Substituting

$$u^f_r = \phi^f_{,r}, \quad u^f_\theta = r^{-1}\phi^f_{,\theta} \text{ and } u^f_z = \phi^f_{,z} \quad (26)$$

and seeking the solution of Eq. (24) in the form

$$\phi^f(r,\theta,z,t) = \sum_{n=0}^{\infty} \phi^f(r) \cos n\theta e^{i(\varsigma\bar{z} + \Omega T_a)} \quad (27)$$

The fluid that represents the oscillatory wave propagating away is given as

$$\phi^f = A_6 H_n^{(1)}(\alpha_6 a x) \quad (28)$$

where $(\alpha_6 a)^2 = \Omega^2/\rho_R \overline{B}^f - \zeta^2$, in which $\rho_R = \rho/\rho^f, \overline{B}^f = B^f/c_{44}$, $H_n^{(1)}$ is the Hankel function of first kind. If $(\alpha_6 a)^2 < 0$, then the Hankel function of first kind is to be replaced by K_n, where K_n is the modified Bessel function of the second kind. By substituting Eq. (27) in Eq. (23) along with Eq. (26), the acoustic pressure for the fluid can be expressed as

$$p^f = \sum_{n=0}^{\infty} A_6 \Omega^2 \bar{\rho} H_n^{(1)}(\alpha_6 ax) \cos n\theta e^{i(\varsigma\bar{z}+\Omega T_a)} \quad (29)$$

5. Boundary conditions and frequency equations

The continuity conditions in a solid–solid interface problem and in case of real fluid problem require three traction free stress component in its surfaces. But, in an ideal fluid-solid interface the perfect slip boundary conditions imply the discontinuity in planar displacement component. That is, the radial component of the displacement of the fluid and solid must be equal at the interfaces; however, the circumferential and longitudinal components are discontinuous and the three surface stresses are equal to zero.

The solid fluid interfacial boundary conditions for infinite cylindrical bar are given by

$$\sigma_{rr} + p^f = \sigma_{r\theta} = \sigma_{rz} = u - u^f = 0, \qquad \text{at } r = a \quad (30)$$

The electrical and magnetic boundary conditions for an infinite cylindrical bar are,

$$D_r = 0 \quad \text{and} \quad B_r = 0 \quad (31)$$

Using Eqs. (19), (22) and (29) in Eqs. (30) and (31), we can obtain the frequency equation in the following form.

$$|M_{ij}| = 0 \quad i,j = 1,2,3,4,5,6. \quad (32)$$

where the elements in the determinant are given as

$$\begin{aligned}
M_{1j} &= 2\bar{c}_{66}[n(n-1)J_n(\alpha_j ax) + (\alpha_j ax)J_{n+1}(\alpha_j ax)] \\
&\quad -x^2[\bar{c}_{11}(\alpha_j ax)^2 + \zeta(a_j\bar{c}_{13} + b_j\bar{e}_{31} + c_j\bar{q}_{31})]J_n(\alpha_j ax),\ j = 1,2,3,4 \\
M_{15} &= 2\bar{c}_{66}[n(n-1)J_n(\alpha_5 ax) + n(\alpha_5 ax)J_{n+1}(\alpha_5 ax)] \\
M_{16} &= \rho^f \Omega^2 H_n^{(1)}(\alpha_6 a) \\
M_{2j} &= 2[n(n-1)J_n(\alpha_j ax) - n(\alpha_j ax)J_{n+1}(\alpha_j ax)],\ j = 1,2,3,4 \\
M_{25} &= [2n(n-1) - (\alpha_5 ax)^2]J_n(\alpha_5 ax) + 2(\alpha_5 ax)J_{n+1}(\alpha_5 ax) \\
M_{26} &= 0 \\
M_{3j} &= (\varsigma + a_j + b_j\bar{e}_{15} + c_j\bar{q}_{15})[nJ_n(\alpha_j ax) - (\alpha_j ax)J_{n+1}(\alpha_j ax)], \\
&\quad j = 1,2,3,4 \\
M_{35} &= n\varsigma J_n(\alpha_5 ax),\ M_{36} = 0 \\
M_{4j} &= [(\varsigma + a_j)\bar{e}_{15} - \bar{\varepsilon}_{11}b_j - \bar{m}_{11}c_j][nJ_n(\alpha_j ax) - (\alpha_j ax)J_{n+1}(\alpha_j ax)] \\
&\quad j = 1,2,3,4 \\
M_{45} &= n\varsigma\bar{e}_{15}J_n(\alpha_5 ax),\ M_{46} = 0 \\
M_{5j} &= ((\varsigma + a_j)\bar{q}_{15} - \bar{m}_{11}b_j - \bar{\mu}_{11}c_j)[nJ_n(\alpha_j ax) - (\alpha_j ax)J_{n+1}(\alpha_j ax)] \\
&\quad j = 1,2,3,4 \\
M_{55} &= n\varsigma\bar{q}_{15}J_n(\alpha_5 ax),\ M_{56} = 0 \\
M_{6j} &= \left\{nH_n^{(1)}(\alpha_j a) - (\alpha_j a)H_{n+1}^{(1)}(\alpha_j a)\right\}, j = 1,2,3,4 \\
M_{65} &= nJ_n(\alpha_5 a) \\
M_{66} &= -\left\{nH_n^{(1)}(\alpha_6 a) - (\alpha_6 a)H_{n+1}^{(1)}(\alpha_6 a)\right\}.
\end{aligned} \quad (33)$$

6. Numerical discussion

In this problem, the free vibration of transversely isotropic magnetoelectroelastic solid bar immersed in fluid is considered. In the solid–fluid interface problems, the normal stress of the bar is equal to the negative of the pressure exerted by the fluid and the displacement component in the normal direction of the lateral surface of the cylinder is equal to the displacement of the fluid in the same direction. These conditions are due to the continuity of the stresses and displacements of the solid and fluid boundaries. Since the inviscid fluid cannot sustain shear stress, the shear stress of the outer fluid is equal to zero. The material properties of the electro-magnetic material based on graphical results of Aboudi [23] are

$c_{11} = 218 \times 10^9\ \mathrm{N/m^2}$, $c_{12} = 120 \times 10^9\ \mathrm{N/m^2}$, $c_{13} = 120 \times 10^9\ \mathrm{N/m^2}$, $c_{33} = 215 \times 10^9\mathrm{N/m^2}$, $c_{44} = 50 \times 10^9\ \mathrm{N/m^2}$, $c_{66} = 49 \times 10^9\ \mathrm{N/m^2}$, $e_{15} = 0$, $e_{31} = -2.5\ \mathrm{C/m^2}$, $e_{33} = 7.5\ \mathrm{C/m^2}$, $q_{15} = 200\ \mathrm{C/m^2}$, $q_{31} = 265\ \mathrm{C/m^2}$, $q_{33} = 345\ \mathrm{C/m^2}$, $\varepsilon_{11} = 0.4 \times 10^{-9}\ \mathrm{C/Vm}$, $\varepsilon_{33} = 5.8 \times 10^{-9}\ \mathrm{C/Vm}$, $\mu_{11} = -200 \times 10^{-6}\ \mathrm{Ns^2/C^2}$, $\mu_{33} = 95 \times 10^{-6}\ \mathrm{Ns^2/C^2}$, $m_{11} = 0.0074 \times 10^{-9}\ \mathrm{Ns/VC}$, $m_{33} = 2.82 \times 10^{-9}\ \mathrm{Ns/VC}$ and $\rho = 7500\ \mathrm{Kg\,m^{-2}}$ and for fluid the density $\rho^f = 1000\ \mathrm{Kg\,m^{-3}}$, phase velocity $c_f = 1500\ \mathrm{m\,s^{-1}}$. The velocity and density ratio between the fluid and solid medium is defined as follows $v_R = \frac{c_1}{c_f}$ and $\rho_R = \frac{\rho}{\rho^f}$.

The complex secular Eq. (33) contains complete information regarding wave number, phase velocity and attenuation coefficient and other propagation characteristics of the considered surface waves. In order to solve this equation we take

$$c^{-1} = v^{-1} + i\omega^{-1}q \quad (34)$$

where $k = R + iq$, $R = \frac{\omega}{v}$ and R,q are real numbers. Here it may be noted that v and q respectively represent the phase velocity and attenuation coefficient of the waves. Upon using the representation Eq. (34) in Eq. (33) and various relevant relations, the complex roots $\alpha_j (j = 1,2,3,4)$ of the quadratic Eq. (17) can be computed with the help of Secant method. The characteristic roots $\alpha_j (j = 1,2,3,4)$ are further used to solve Eq. (33) to obtain phase velocity (v) and attenuation coefficient (q) by using the functional iteration numerical technique as given below.

Eq. (33) is of the form $F(C) = 0$ which upon using representation Eq. (34) leads to a system of two real equations $f(v,q) = 0$ and $g(v,q) = 0$. In order to apply functional iteration method, we write $v = f^*(v,q)$ and $q = g^*(v,q)$, where the functions f^* and g^* are selected in such a way that they satisfy the conditions

$$\left|\frac{\partial f^*}{\partial v}\right| + \left|\frac{\partial g^*}{\partial q}\right| < 1, \quad \left|\frac{\partial g^*}{\partial v}\right| + \left|\frac{\partial f^*}{\partial q}\right| < 1 \quad (35)$$

For all v, q in the neighborhood of the roots. If (v_0, q_0) be the initial approximation of the root, then we construct a successive approximation according to the formulae

$$\begin{aligned}
v_1 &= f^*(v_0, q_0) & q_1 &= g^*(v_1, q_0) \\
v_2 &= f^*(v_1, q_1) & q_2 &= g^*(v_2, q_1) \\
v_3 &= f^*(v_2, q_2) & q_3 &= g^*(v_3, q_2) \\
&\cdots\cdots & &\cdots\cdots \\
v_n &= f^*(v_n, q_n) & q_n &= g^*(v_{n+1}, q_n)
\end{aligned} \quad (36)$$

The sequence $\{v_n, q_n\}$ of approximation to the root will converge to the actual value (v_0, q_0) of the root provided (v_0, q_0) lie in the neighborhood of the actual root. For the initial value $c = c_0 = (v_0, q_0)$, the roots $\alpha_j (j = 1,2,3,4)$ are computed from Eq. (17) by using Secant method for each value of the wave number k, for assigned frequency. The values of α_j $(j = 1,2,3,4)$ so obtained are then used in Eq. (33) to obtain the current values of v and q each time which are further used

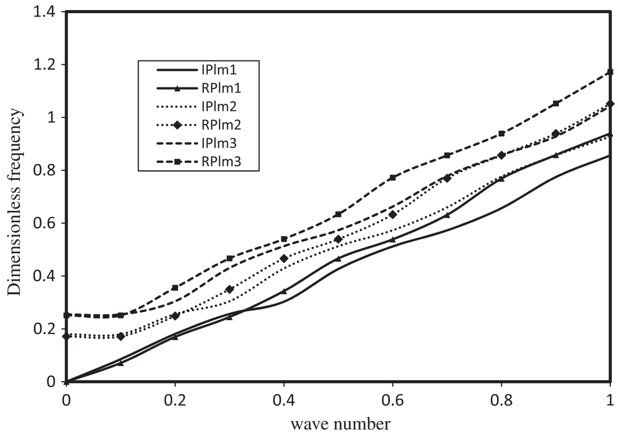

Figure 1 Dimensionless frequency Ω versus wave number $|\varsigma|$ of longitudinal modes of vibration for a magneto-electro elastic solid bar with $v_R = 0.5$.

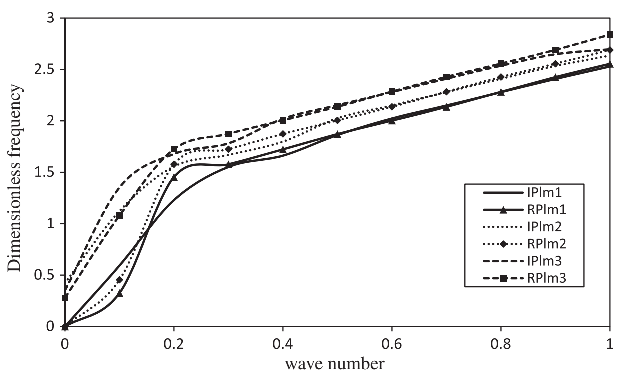

Figure 2 Dimensionless frequency Ω versus wave number $|\varsigma|$ of longitudinal modes of vibration for a magneto-electro elastic solid bar with $v_R = 1.0$.

to generate the sequence Eq. (36). This process is terminated as and when the condition $|v_{n+1} - v_n| < \varepsilon, \varepsilon$ being arbitrary small number to be selected at random to achieve the accuracy level, is satisfied. The procedure is continually repeated for different values of the wave number (k) to obtain the corresponding values of the phase velocity(c) and attenuation coefficient (q).

6.1. Dispersion curves

The results of imaginary part and real part of longitudinal modes are plotted in the form of dispersion curves. The notation used in the figures, namely IPlm and RPlm respectively denotes the imaginary part of longitudinal mode and real part of longitudinal, The 1 refers the first mode, 2 refers the second mode and 3 for the third mode.

In Figs. 1 and 2 the variations in the non-dimensional frequency Ω of a elastic cylindrical bar with respect to the wave number $|\varsigma|$ have been shown for first three modes of imaginary and real part of longitudinal vibrations for the bar immersed in fluid with the velocity ratio $v_R = 0.5$, 1.0. From Fig.1, it is observed that the non-dimensional frequency of the electromagnetic bar shows almost linear variation with respect to wave number for the velocity ration $v_R = 0.5$. But in Fig. 2 some oscillating nature is observed between $0 \leqslant |\varsigma| \leqslant 2$ from the linear behavior of frequency due to the damping effect of surrounding fluid medium and increase in velocity ratio is more prominent in lower wave number. From Figs. 1 and 2, it is observed that the imaginary part of the frequency mode is less compared with real part due to damping of fluid medium.

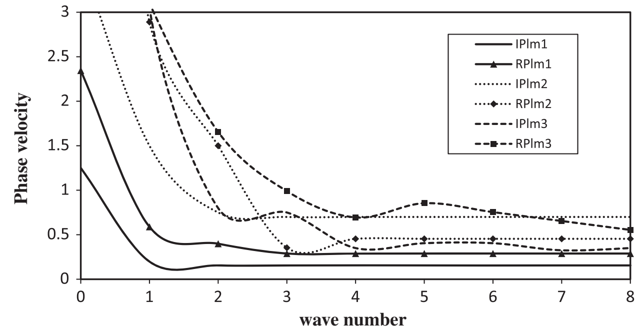

Figure 3 Phase velocity c versus wave number $|\varsigma|$ of longitudinal modes of vibration for a magneto-electro elastic solid bar with $v_R = 0.5$.

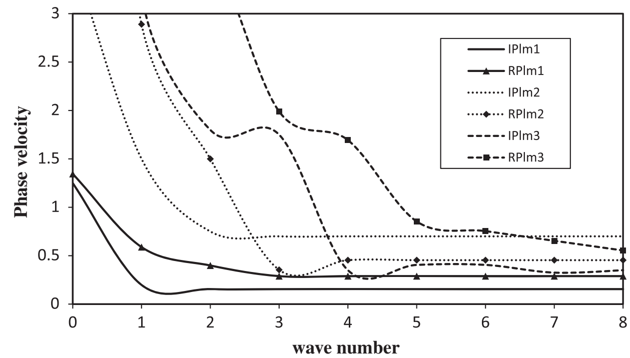

Figure 4 Phase velocity c versus wave number $|\varsigma|$ of longitudinal modes of vibration for a magneto-electro elastic solid bar $v_R = 1.0$.

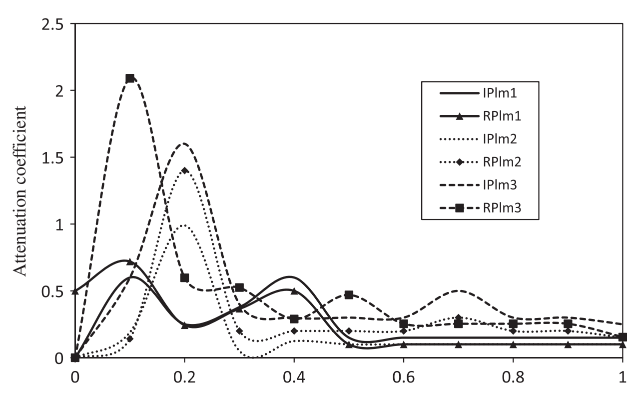

Figure 5 Attenuation coefficient q versus wave number $|\varsigma|$ of longitudinal modes of vibration for a magneto-electro elastic solid bar with $v_R = 0.5$.

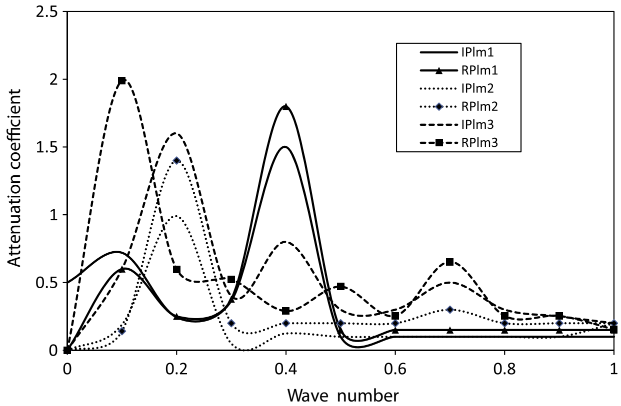

Figure 6 Attenuation coefficient q versus wave number $|\varsigma|$ of longitudinal modes of vibration for a magneto-electro elastic solid bar with $v_R = 1.0$.

The variation in the phase velocity with respect to the wave number of the cylindrical bar in with the velocity ratio $v_R = 0.5$, 1.0 is shown in Figs. 3 and 4, respectively. From these curves it is clear that the phase velocity curves are dispersive only at the starting values of wave number in the range $0 \leqslant |\varsigma| \leqslant 0.4$ in Fig. 3 and $\leqslant |\varsigma| \leqslant 0.5$ in Fig. 4, but for higher values of wave number, these become non-dispersive for both the values of the velocity ratio $v_R = 0.5$ and $v_R = 1.0$. But there is a small dispersion of cutoff frequency in $v_R = 1.0$ which might happen because of the radiation of the sound energy in to the fluid produces damping in the system. The phase velocity of real and imaginary modes of propagation attains quite large values at vanishing wave number which sharply slashes down to become steady and asymptotic with increasing wave number.

The dispersion of attenuation coefficient q with respect to the wave number $|\varsigma|$ is discussed for the two cases of immersed and free magnetoelectro elastic solid bar in Figs. 5 and 6. The amplitude of displacement of the attenuation coefficient increases monotonically to attain maximum value in $0.4 \leqslant q \leqslant 0.8$ and slashes down to became asymptotically linear in the remaining range of the wave number in Fig. 5. The variation in attenuation coefficient for different real and imaginary parts of longitudinal modes is oscillating in the maximum range of wave number as shown in Fig. 6. From Figs. 5 and 6, it is clear that the attenuation profiles exhibit high oscillating nature in the velocity ratio $v_R = 1.0$ than $v_R = 0.5$ due to the combined effect of magnetic fields and surrounding fluid. The crossover points in the vibrational modes indicate the energy transfer between the solid and fluid medium.

7. Conclusion

In this paper, the wave propagation in a magneto-electro-elastic solid bar immersed in fluid is analyzed within the frame work of three dimensional liner theory of magneto-electro elastic by satisfying the traction free and perfect slip boundary conditions. The frequency equation is obtained using Bessel functions and numerically analyzed for the solid bar with different velocity ratios. The computed dimensionless frequency, phase velocity and attenuation coefficient are plotted in graphs for the real and imaginary part of longitudinal modes of vibrations. From the numerical results, it is observed that the increase in velocity ratio and the presence of fluid medium influence all the modes of frequency, phase velocity and attenuation. Also it is observed that as wave number increases the imaginary part of the vibration modes decreases, which exhibits the proper physical behavior. The obtained results are valuable for the analysis of design of magneto-electric transducer and sensors using composite materials.

References

[1] E. Pan, Exact solution for simply supported and multilayered magneto-electro-elastic plates, Trans. ASME. 68 (2001) 608–618.
[2] E. Pan, P.R. Heyliger, Free vibration of simply supported and multilayered magneto-electro-elastic plates, J. Sound Vib. 252 (2002) 429–442.
[3] E. Pan, P.R. Heyliger, Exact solutions for magneto-electro-elastic laminates in cylindrical bending, Int. J. Solid Struct. 40 (2003) 6859–6876.
[4] E. Pan, F. Han, Exact solution for functionally graded and layered magneto-electro-elastic plates, Int. J. Eng. Sci. 43 (2005) 321–339.
[5] W.J. Feng, E. Pan, Dynamic fracture behavior of an internal interfacial crack between two dissimilar magneto-electro-elastic plates, J. Eng. Fract. Mech. 75 (2008) 1468–1487.
[6] G.R. Buchanan, Free vibration of an infinite magneto-electro-elastic cylinder, J. Sound Vib. 268 (2003) 413–426.
[7] H.L. Dai, X. Wang, Thermo-electro-elastic transient responses in piezoelectric hollow structures, Int. J. Solid Struct. 42 (2005) 1151–1171.
[8] H.L. Dai, X. Wang, Magneto-thermo-electro-elastic transient response in a piezoelectric hollow cylinder subjected to complex loadings, Int. J. Solid Struct. 43 (2006) 5628–5646.
[9] T. Kong, D.X. Li, X. Wang, Thermo-magneto-dynamic stresses and perturbation of magnetic field vector in non-homogeneous hollow cylinder, Appl. Math. Modelling 33 (2009) 2939–2950.
[10] A.R. Annigeri, N. Ganesan, S. Swarnamani, Free vibration of clamped-clamped magneto-electro-elastic cylindrical shells, J. Sound Vib. 292 (2006) 300–314.
[11] A.R. Annigeri, N. Ganesan, S. Swarnamani, Free vibration behavior of multiphase and layered magneto-electro-elastic beam, J. Sound Vib. 299 (2007) 44–63.
[12] A.R. Annigeri, N. Ganesan, S. Swaranmani, Free vibrations of simply supported layered and multiphase magneto-electro-elastic cylindrical shells, Smart Mater. Struct. 15 (2006) 459–467.
[13] P.F. Hon, A.Y. Leung, H.J. Ding, A point heat source on the surface of a semi-infinite transversely isotropic electro-magneto-thermo-elastic material, Int. J. Eng. Sci. 46 (2008) 273–285.
[14] J.N. Sharma, Mohinder Pal, Rayleigh-Lamb waves in magneto-thermoelastic homogeneous isotropic plate, Int. J. Eng. Sci. 42 (2004) 137–155.
[15] J.N. Sharma, M.D. Thakur, Effect of rotation on Rayleigh-Lamb waves in magneto-thermoelastic media, J. Sound Vib. 296 (2006) 871–887.
[16] G.F. Gao, N. Noda, Thermal-induced interfacial cracking of magnetoelectroelastic materials, Int. J. Eng. Sci. 42 (2004) 1347–1360.
[17] W. Bin, Y. Jiangong, H. Cunfu, Wave propagation in non-homogeneous magneto-electro-elastic plates, J. Sound Vib. 317 (2008) 250–264.
[18] K. Sinha, J. Plona, S. Kostek, S. Chang, Axisymmetric wave propagation in a fluid-loaded cylindrical shell. I: Theory; II theory versus experiment, J. Acoust. Soc. Am. 92 (1992) 1132–1155.

[19] J. Berliner, R. Solecki, Wave Propagation in a fluid-loaded, transversely isotropic cylinder. Part I. Analytical formulation; Part II Numerical results, J. Acoust. Soc. Am. 99 (1996) 1841–1853.

[20] P. Ponnusamy, Wave propagation in a generalized thermoelastic solid cylinder of arbitrary cross-section immersed in a fluid, Int. J. Mech. Sci. 49 (2007) 741–751.

[21] P. Ponnusamy, R. Selvamani, Wave propagation in a magneto thermo elastic cylindrical panel, Eur. J. Mech. A/Solid 39 (2013) 76–85.

[22] P. Ponnusamy, R. Selvamani, Dispersion analysis of a generalized magneto thermo elastic cylindrical panel, J. Therm. Stresses 35 (12) (2012) 1119–1142.

[23] J. Aboudi, Micromechanical analysis of fully coupled electro-magneto-thermo-elastic multiphase composites, Smart Mater. Struct. 10 (2001) 867–877.